colloids and interfaces

MDPI

Article

Examination of a Theoretical Model for Drainage of Foams Prepared from Licorice Root Extract Solution

Hashem Ahmadi Tighchi [1], Mohammad Hasan Kayhani [1,*], Ali Faezian [2], Samira Yeganehzad [3] and Reinhard Miller [4]

[1] Faculty of Mechanical and Mechatronics Engineering, Shahrood University of Technology, Shahrood P.O. Box 3619995161, Iran; hashem.ahmadi@shahroodut.ac.ir
[2] Department of Food Machinery Design, Research Institute of Food Science & Technology (RIFST), Mashhad P.O. Box 91895157356, Iran; a.faezian@rifst.ac.ir
[3] Department of Food Processing, Research Institute of Food Science & Technology (RIFST), Mashhad P.O. Box 91895157356, Iran; s.yeganehzad@rifst.ac.ir
[4] Physics Department, Technical University Darmstadt, 64289 Darmstadt, Germany; reinhard.miller@pkm.tu-darmstadt.de
* Correspondence: h_kayhani@shahroodut.ac.ir

Abstract: The root of the licorice plant (Glycyrrhiza glabra) is rich in natural surfactants, called saponins. The beneficial properties of this plant have led to different applications, including its use as a foaming agent. In this research, a theoretical model and its validity are discussed for the liquid drainage of foams made from licorice root extract solutions. After stating the important characteristics in the free drainage of foam, a relationship of the drained liquid volume based on effective parameters was obtained via a simplification of the governing equation. The theoretical model is applied to experimental foam drainage data measured at different concentrations of licorice root extract solutions. A comparison of theoretical and experimental results shows good agreement for the volume of drained liquid as a function of time. The characteristics obtained from the combination of effective parameters allows for a quantification of the drainage rate. In addition, the drainage rate at the beginning of the foam decay process, as a measure of stability, can be estimated using measurable properties.

Keywords: licorice root extract; theoretical model; free drainage; foam; liquid flow

Citation: Ahmadi Tighchi, H.; Kayhani, M.H.; Faezian, A.; Yeganehzad, S.; Miller, R. Examination of a Theoretical Model for Drainage of Foams Prepared from Licorice Root Extract Solution. *Colloids Interfaces* **2023**, *7*, 47. https://doi.org/10.3390/colloids7020047

Academic Editor: Akmal Nazir

Received: 30 April 2023
Revised: 11 June 2023
Accepted: 12 June 2023
Published: 14 June 2023

1. Introduction

Foams are widely used in daily life and industry due to their unique properties. Foam applications include cleaning, food, pharmaceuticals, cosmetics, building materials, and petroleum. During the preparation of foam as a colloidal system, various mechanisms are involved in its production and stabilization, such as the formations of bubbles and liquid films, the coarsening of the foam, the rupture of liquid films, and the liquid drainage due to gravity. The stability of foams is a crucial factor for their successful use. Three types of mechanisms cause the breakage of aqueous foams: (i) foam drainage due to gravity and capillarity, (ii) coarsening due to gas transfer between bubbles because of capillary pressure differences, and (iii) bubble coalescence due to rupture of films formed among bubbles [1]. The coarsening process indirectly controls the stability of the foam, so that the coarsening rate is related to the liquid volume fraction inside the foam [2,3]. Therefore, foam drainage and coarsening are interdependent. In general, among these three mechanisms, foam drainage, which refers to the liquid fraction of foams, is the main parameter for both bubble coalescence and coarsening processes [4]. Accordingly, theories of foam drainage have been investigated during recent decades and methods have been examined to monitor the drainage rate.

Drainage is the result of the liquid flow in the films and channels formed between the bubbles. The foam drainage equation is a theoretical model for the dynamics of the liquid

flow, considering the effects of gravity, capillary pressure, and viscous resistance [5,6]. The flow in foams and liquid drainage have been investigated, from experimental and theoretical points of view, for different situations, including free drainage [7–9], where the liquid of an initial uniform foam emerges at the bottom, forced drainage [10–12], where the liquid is added to the top of the foam column, the wetting of a dry foam [13,14], and pulse drainage [5,15,16]. It has been shown that, in addition to the liquid volume fraction, parameters such as surface tension, solution viscosity, liquid density, bubble size, and the initial foam height affect the drainage rate and, consequently, the foam stability.

Surfactants have great potential as foaming agents, due to their high surface activity in aqueous solutions. Licorice root is a useful plant and a rich source of natural surfactants (saponins). Today, because of the many benefits that natural surfactants provide, such as availability, degradability, renewability, and positivity for health, the tendency to use them has expanded. The root of licorice (Glycyrrhiza glabra) contains glycyrrhizin saponin and is frequently used in food and medicine and in the detergent industry. The licorice root extract (LRE) mainly consists of triterpenoid glycoside glycyrrhizin, sugars, saponins, flavonoids, sterols, gums, amino acids, starches, and essential oils [17,18]. Licorice root was traditionally used to treat or prevent many diseases in which free radicals or oxidants are involved [19]. It was also found that LRE has other beneficial pharmacological properties, such as being antiviral, antioxidative, anti-inflammatory, anticancer, and antimicrobial [20,21]. Several studies have indicated that LRE can be used as an ingredient in the food industry, not only as a sweetener but also as foaming or emulsifying agent, especially in cakes or beverages [22–25]. To date, there have been very limited studies on the foam behavior of licorice extract [26–28]. Hence, very little progress has been made in elucidating a relationship for foam drainage prepared from LRE solutions. By providing a simple model based on effective parameters, the drainage rate and foam stability can be estimated, which helps experts in using this foam more efficiently.

The present paper examines a simplified theoretical model for the description of liquid drainage from foams made of solutions of LRE used as foaming agent. The parameters affecting the foam drainage were determined via a mathematical method. Then, for the experimental approach, solutions were studied in a broad concentration range. By comparing the theoretical and experimental results as a validation of the model, the effective properties were quantified. In this way, suitable relationships based on measurable quantities are provided to estimate the stability of LRE foams.

2. Theoretical Model

2.1. Drainage Equation

In past decades, the dynamics of foam drainage were extensively studied. Generally, the scales of such studies were greater than a consideration of individual bubbles; i.e., the liquid fraction was more thoroughly considered in quantifying the drainage of aqueous foams (a continuum approach). Accordingly, the drainage equation has been a popular model for describing the liquid flow in the channel-like network of foams as a function of time. In aqueous foams, the liquid flow occurs via three paths: the films between two neighboring bubbles, the junctions of three adjoining films called the Plateau border channel, and the junctions of four Plateau borders, called nodes (see Figure 1). Two principal assumptions were considered to derive the drainage equation in the standard form. The first assumption was that the effects of liquid flow in films are negligible, so the drainage occurs through the Plateau borders. The second assumption was that the liquid flow is inside a rigid channel; i.e., a no-slip boundary condition was supposed. In fact, a Poiseuille flow was assumed in the channels formed between the bubbles. It has been recommended that an assumption be made that the liquid flow in foams is analogous to the flow through a porous medium such as a solid sphere [5,29]. In this way, the dissipation can be described using Darcy's law.

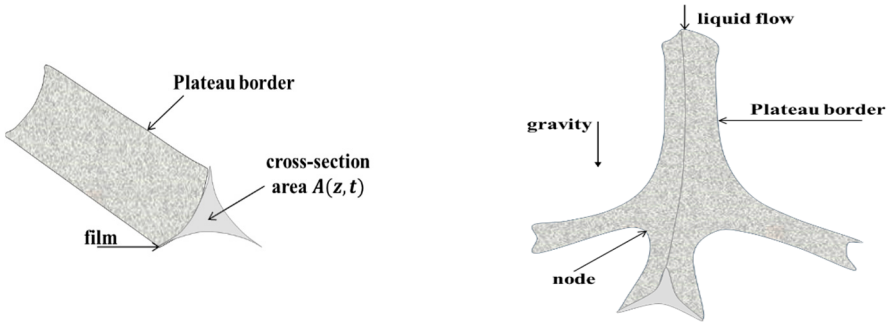

Figure 1. (**a**) Schematic of a Plateau border channel. (**b**) Schematic of a node (meeting at a four-fold junction).

Below, the driving standard drainage equation is reviewed. To derive the drainage equation, the volume fraction of liquid, $\varepsilon(z,t)$, along the foam and as a function of time, is estimated by the cross-sectional area of the Plateau borders $A(z,t)$, which depends on the vertical downward position z and time t. This is because the liquid flow occurs through the channels; thus, the area cross-section of the Plateau borders determines the local liquid fraction. Therefore, the continuity equation for the conservation law can be expressed as follows:

$$\frac{\partial A}{\partial t} + \frac{\partial}{\partial z}(uA) = 0 \tag{1}$$

To better understand this equation, a Plateau border channel is first considered in a vertical orientation. The area of a cross-section can be evaluated using the radius of sphere-equivalent bubbles. The triangular area formed between three circles is considered the cross-section of a channel and is obtained by the following equation:

$$A = C^2 {r_c}^2 \tag{2}$$

where $C = \sqrt{3} - \pi/2 = 0.161$ and r_c is the radius of curvature, which is related to the gas pressure inside the bubbles and the liquid pressure in the channels. This law is defined by the Young–Laplace equation as

$$p_g - p_l = \frac{\gamma}{r_c} \tag{3}$$

where p_l, p_g, and γ are liquid pressure, gas pressure, and surface tension, respectively. On the other hand, the velocity of the liquid flow u inside the Plateau borders is determined by the interaction of three effects: the gravitational force, the viscous dissipation, and the pressure gradient because of the lower-pressure liquid. By considering a Stokes flow for the liquid motion in the plateau borders, the relationship between the mentioned terms can be expressed by the following equation:

$$\rho g + (-\nabla p) + \mu \nabla^2 u = 0 \tag{4}$$

Here. ρg is the gravity term, $-\left(\frac{\partial}{\partial z}\right) p_l = -\left(\frac{\partial}{\partial z}\right)\left(\frac{\gamma}{r_c}\right)$ is the capillary pressure, and the third term is the viscous dissipation, which is estimated by $-\frac{\mu u}{A}$. The viscosity μ depends on the liquid viscosity μ_l through the coefficient, which is determined by the channel shape (its value is 50 for the Plateau borders) [22]. Accordingly, the velocity u is obtained through the following equation as a function of A:

$$u = \frac{1}{\mu}\left(\rho g A - \frac{C\gamma}{2\sqrt{A}}\frac{\partial A}{\partial z}\right) \tag{5}$$

The standard drainage equation is obtained from the combination of the velocity relation and the continuity equation to calculate $A(z,t)$ as follows:

$$\frac{\partial A}{\partial t} + \frac{1}{\mu}\frac{\partial}{\partial z}\left(\rho g A^2 - \frac{C\gamma}{2}A^{1/2}\frac{\partial A}{\partial z}\right) = 0 \tag{6}$$

As stated above, this equation was derived by assuming vertical channels. In reality, however, the Plateau borders point in different directions. Therefore, the coordinate should be modified in the direction of the tilted channel, as $z_\theta = zcos\theta$. In addition, the gravitational force must be multiplied by $cos\theta$. Consequently, the drainage equation may be rewritten in the following form:

$$\frac{\partial A}{\partial t} + \frac{cos^2\theta}{\mu}\frac{\partial}{\partial z}\left(\rho g A^2 - \frac{C\gamma}{2}A^{1/2}\frac{\partial A}{\partial z}\right) = 0 \tag{7}$$

In order to consider the influence of all channels in different directions, the average of $cos^2\theta$ must be considered $\left(\langle cos^2\theta\rangle = 1/3\right)$. In this way, it is possible to define an effective viscosity that takes into account the dissipation of the liquid flow in the network of all Plateau borders. Thus, we obtain an effective viscosity $\mu^* = 3\mu = 150\mu_l$ which is applied in the drainage equation to consider a realistic network. In conclusion, the section area of the Plateau borders $A(z,t)$ can be computed by solving the nonlinear partial differential equation. Subsequently, the liquid volume fraction $\varepsilon(z,t)$ is evaluated along the foam as a function of time. Different methods for solving this equation have been stated and various experiments have been conducted and compared with these theoretical solutions [13,30–33].

2.2. Free Drainage

In the present study, the drainage of a uniform foam column with a height h is discussed, produced by the Bikerman method [34,35]. This problem is called free drainage, which indicates the stability of the initial uniform foam. Most researchers tend to transform the drainage equation into a dimensionless form using characteristic parameters. This work has two main advantages: first, solving the equation will be easier, and second, the discussion of the results will be more practical. The following dimensionless parameters for rewriting the drainage equation were proposed by Koehler et al. [6] using the bubble radius R:

$$A(z,t) = C^2R^2\alpha(\xi,\tau),\ z = \frac{\gamma}{2\rho g R}\xi,\ t = \frac{\mu^*\gamma}{2C^2R^3(\rho g)^2}\tau \tag{8}$$

where τ and ξ are dimensionless time and height, respectively. Therefore, the non-dimensional form of the standard drainage equation is described as follows:

$$\frac{\partial \alpha}{\partial \tau} + \frac{\partial \alpha^2}{\partial \xi} - \frac{\partial}{\partial \xi}\left(\alpha^{1/2}\frac{\partial \alpha}{\partial \xi}\right) = 0 \tag{9}$$

Since foam drainage modeling led to a partial differential equation, boundary conditions are needed to solve the equation. At $\xi = 0$ (i.e., at the foam top), zero flow is applied, which agrees with the free drainage condition.

$$\alpha^{3/2}(\tau) - \frac{\partial}{\partial \xi}\alpha(\tau) = 0 \tag{10}$$

The foam is in contact with liquid at the bottom. Accordingly, the following approximation is defined for this boundary:

$$\alpha(\tau) = 1 \tag{11}$$

It should be noted that there is still an issue related to the drainage equation; i.e., the location of the viscous dissipation. In other words, the boundary condition of liquid flow

at the channel wall is an important assumption that can affect the equation and, hence, the simulation of the drainage process. Therefore, the boundary walls of the Plateau border channels can also be considered more mobile (a plug flow assumption); accordingly, viscous dissipation can happen because of the bending of the streamlines inside the nodes. For this condition, the scaling of $A^{0.5}$ is set in the velocity relation rather than A. As a result, two boundary conditions are possible for the Plateau border: no-slip and free-slip conditions, which identify a Poiseuille flow and plug flow, respectively. Finally, the standard drainage equation can be expressed as follows:

$$\frac{\partial \alpha}{\partial \tau} + \frac{\partial}{\partial \xi}\left(\alpha^{m+1} - \frac{1}{2m+1}\frac{\partial \alpha^{m+1/2}}{\partial \xi}\right) = 0 \tag{12}$$

where the index m is 1 for the no-slip condition (border-dominated flow) and $1/2$ for the free-slip condition (nodes-dominated flow), with a shear flow within the junctions.

2.3. Solution of the Free Drainage Equation

As stated above, the present objective is to solve the free drainage in a foam column with a constant cross-sectional area $A(z,0) = A_0$. An analytical solution for the free drainage problem was derived by Kraynik [24] and Saint-Jalmes [11]; however, they neglected the capillarity term to decrease the nonlinearity in the standard drainage equation. This simplification is acceptable when the foam height is a very large scale, i.e., $h \gg \zeta$, where ζ is the capillary rise height for the liquid:

$$\zeta = \frac{C\gamma}{2\rho g\sqrt{A_h}} \tag{13}$$

Through this approximation, the partial differential equation transforms into a first-order equation and zero-flow can be assumed at the top layer for the required boundary condition. Using this simplification, the following explicit solution is obtained:

$$A(z,t) = A_0\begin{cases}\left(\frac{z}{u_0 t}\right)^{1/m} & z \le u_0 t \\ 1 & z \ge u_0 t\end{cases} \tag{14}$$

It can be observed that the solution of the equation depends on the viscous dissipation mechanism through the index m. In addition, u_0 denotes the maximum characteristic velocity related to the drying propagation starting from the foam top and depends on the initial area, as defined below:

$$u_0 = \frac{2\rho g A_0}{\mu^*} \tag{15}$$

Therefore, the time-dependent liquid fraction along the foam starting from an initial value ε_0 is determined by the following equation:

$$\varepsilon(z,t) = \varepsilon_0\begin{cases}\left(\frac{z}{vt}\right)^{1/m} & z \le vt \\ 1 & z \ge vt\end{cases} \tag{16}$$

where v is a constant velocity and is expressed by

$$v = u_0(m+1)\varepsilon_0^m \tag{17}$$

It can be concluded that the initial liquid volume fraction and the flow boundary conditions in the Plateau borders determine the velocity of the drying front. Therefore, in order to quantify the interpretation of the foam drainage behavior and to predict the amount of drained liquid, it is necessary to determine the physical properties of the used solution and the initial liquid content inside the foam. According to the equation for the liquid volume fraction, for channel viscous dissipation and junction viscous dissipation,

the liquid distribution is linear and quadratic, respectively, near the upper boundary, while the liquid profile is constant near the bottom boundary. In the present work, experiments were performed to examine the drainage behavior by measuring the drained liquid volume accumulated below the foam bottom. For a better comparison, using the integration of the liquid fraction relation along the foam height, the drained liquid volume may be computed as a function of time via

$$\frac{V(t)}{V_f} = \begin{cases} \frac{1}{m+1}\left(\frac{vt}{h}\right) & vt \le h \\ 1 - \frac{m}{m+1}\left(\frac{h}{vt}\right)^{1/m} & vt \ge h \end{cases} \quad (18)$$

Here, V_f represents the final volume of liquid that is drained. According to this relation, the behavior of the drained liquid volume consists of two parts as a function of time. For both cases of viscous dissipation in channels or junctions, it is found that the drainage rate is initially linear and high, while over time, the drainage rate reduces and its behavior follows a power law. The curve of the normalized volume is determined by $t = h/v$. The advantages of this relationship are its sufficient accuracy, simplicity, and inclusion of effective parameters that make the results practically useful. Verification of this simplified theoretical model can be examined via a comparison of the computed results with the experimental data. As a result, a model can be proposed that describes the drainage behavior of the LRE foams in terms of measurable and effective parameters.

3. Experiment

3.1. Materials and Solution Preparatios

For preparing aqueous solutions to make foam, pure deionized water was provided from Samen Pharmaceutical Co. (Mashhad, Iran) and stored in proper glass bottles. The root extract of licorice (*Glycyrrhiza glabra*) was supplied by Herbalexsir Co. (Mashhad, Iran). The extract for this study was prepared by using an aqueous extraction procedure [36]. The extract was then dried by a spray dryer (Buchi B-191, Flawil, Switzerland) at 150 °C and kept in air-tight bags until the experiment. The obtained powder contained 11.85 wt% saponins, 3.26 wt% ashes, 0.14 wt% fat, 6.58 wt% moisture content, 76.46 wt% carbohydrates, 1.71 wt% protein, and other compounds in minor amounts. Amounts of protein, fat, carbohydrate, moisture, and ash were measured by the AOAC (2005) official method. In addition, saponin content was obtained using high-performance liquid chromatography (HPLC) at 25 °C. More details in this regard are provided in reference [23].

The solutions were prepared at different LRE concentrations (0.01–0.175 wt%). To create the aqueous solution for measurements, the provided powder was first weighted by a balance (BSA323S CW, Sartorius, Göttingen, Germany) in high precision; then, deionized water was added to reach the desired concentration. Finally, the dissolution was supported by a magnetic stirrer.

3.2. Measurement of Physical Quantities

The solution density at different concentrations was determined using a density meter K1HDDX device (Krüss K100 GmbH, Hamburg, Germany). The surface tension of the solutions was measured using the pendant drop method described in [37] at 25 °C. The solution viscosity was determined with a programmable rotational viscometer (DV III ULTRA, Brookfield Engineering Laboratories, Middleborough, MA, USA) by a ULA model of LV spindle at 25 °C. For this purpose, the cylinder of the viscometer containing 20 mL of the solution was loaded and the outputs were obtained for a shear rate of 100 1/s. Measurements were accomplished in triplicate to obtain data accuracy.

3.3. Bubble Size Analysis

The bubble size distribution was performed with images of freshly formed foam captured using a digital microscope (1600×, Bysameyee, Shenzhen, China) and images were transferred to a data acquisition computer. It should be noted that for this recording,

photos were taken immediately after the foaming process was finished. The Image J software [38] was utilized to find bubble size and, consequently, the size distribution.

3.4. Drainage Measurments

The Bikerman-type method was utilized to produce aqueous foams from the prepared solutions [34]. The gas injection into a solution surfactant is a common way to create a uniform foam. The experimental set-up is displayed schematically in Figure 2. Foams were formed from the LRE solution of 20 mL in a glass column employing air injection at a specific flow rate through a sintered disc placed at the bottom of the cylinder. The height and inside diameter of the column were 50 cm and 4.5 cm, respectively. The pore sizes of the sintered glass filter (G4) were 5–15 micron. The injection flow was set using a ball flow meter which was calibrated in the range of 1–20 L/min for air. The foam drainage was started to be measured at a flow rate of 10 L/min for all solutions to keep the same condition. The amount of drainage was obtained by monitoring and recording the foam height as well as the drained liquid collected at the bottom as a function of time after the injection was finished [35]. Drainage measurements were continued until a negligible value of the foam height remained.

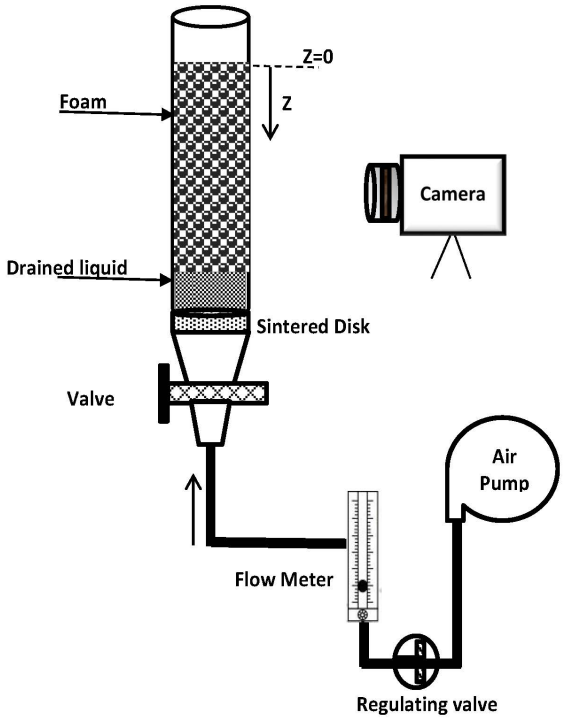

Figure 2. Schematic of the experimental setup for the drainage measurement.

4. Results and Discussions

4.1. Measurements of Effective Parameters

The physical properties, including density, viscosity, and surface tension, that affect the foam drainage, as shown earlier, are presented in Table 1 for LRE solutions at various concentrations ranging from 0.01 to 0.175 wt%. The results showed that the density of LRE solutions slightly increased with the increase in LRE concentration. The surface tension of the LRE solutions reduced noticeably with increasing the extract concentration, as expected. In addition, an increase in the apparent viscosity was observed in response to the increase in the amount of extract dissolved in the solution. Therefore, the maximum viscosity was obtained at the highest concentration.

Table 1. Density, viscosity, and surface tension of LRE solutions.

LRE Concentration (wt%)	Density (kg/m^3)	Viscosity (mPa.s)	Surface Tension (mN/m)
0.01	997.26	1.02	65.17
0.025	997.37	1.03	59.92
0.05	997.43	1.03	56.57
0.075	997.51	1.04	51.47
0.1	997.74	1.04	50.02
0.125	997.81	1.05	49.22
0.15	997.92	1.06	48.87
0.175	998.05	1.08	48.77

As stated in Section 3, the bubble-size distribution of the produced foams was examined via a digital microscope. Figure 3 demonstrates the initial bubble size for three different concentrations of LRE from low to high, as an example. From this figure, it was observed that increasing the concentration of the extract, i.e., increasing the amount of surfactant in the solution, led to a smaller initial size of the bubbles and, hence, a significantly larger number of bubbles. In addition, the increase in the bubble numbers was accompanied by the fact that the bubble size became more homogenous, which can be seen in the photo of the highest concentration (Figure 3c). Since the presence of surfactants in the solution reduces the surface tension, it was expected that the foamability would be improved and the number of bubbles increased at higher LRE concentrations.

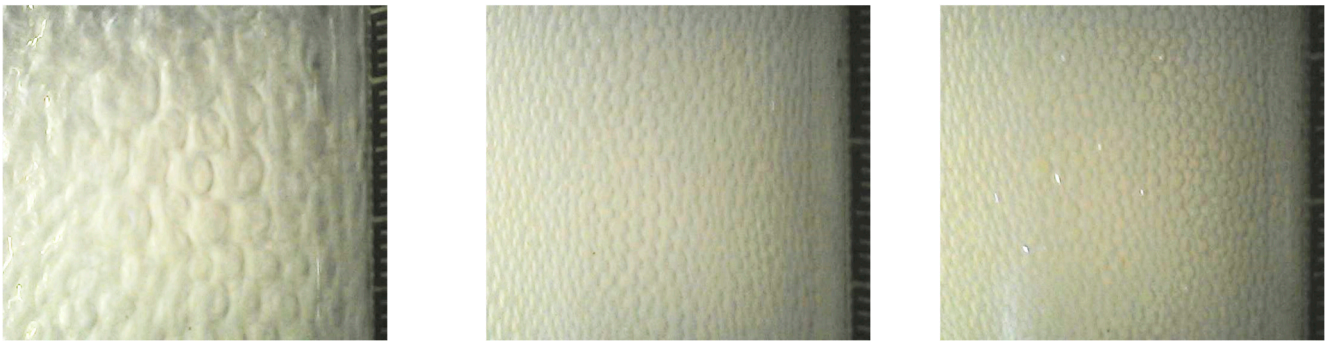

(**a**) (**b**) (**c**)

Figure 3. Photos of the bubble-size distribution for foams at LRE concentrations of (**a**) 0.01 wt%, (**b**) 0.075 wt%, and (**c**) 0.15 wt%.

In the present study, given that the bubbles were nearly spherical, the mean bubble diameter was computed by surface area obtained from the bubble size distribution, as presented in previous literature [39,40]. Therefore, assuming that the bubbles were spherical, the mean equivalent diameter *De* was determined using the surface area of each bubble, as provided using image processing. For example, the diameter distribution of the LRE foam prepared from a 0.15%wt solution is provided in Figure 4. This figure shows that bubble sizes varied from 0.8 to 1.6 mm, although the diameter of most bubbles ranged from 1.1 to 1.4 mm. In addition, it was observed that the maximum bubble size was about 1.1 mm, followed by 1.3 and 1.4 mm. Finally, the mean bubble diameter of this foam was determined to be 1.32 mm.

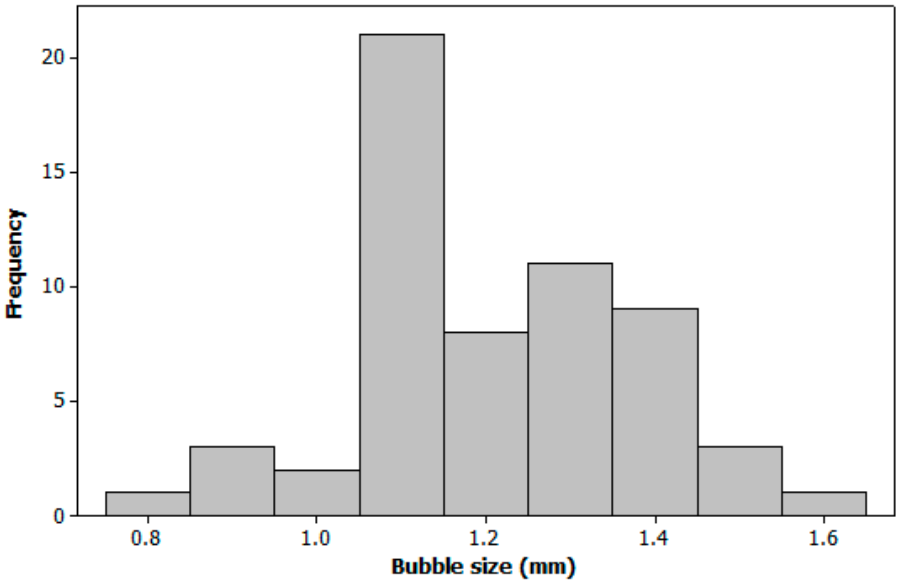

Figure 4. Initial distribution of bubble size for LRE foam at 0.15 wt%.

The average radius of bubbles obtained from image analysis, with error bars representing 90% confidence intervals for each studied foam, is displayed in Figure 5. Generally, as previously mentioned, the average equivalent radius decreased with increasing extract concentration due to lower surface tension. Hence, we can conclude that the decrease in bubble radius correlates with the surface tension reduction so that the average size of bubbles is smaller at higher concentrations ($C \geq 0.1$ wt%) due to the coverage of the bubble surfaces by surfactant molecules. It is also clear that samples with smaller and closely packed bubbles have a lower average radius. The initial average radius of each LRE foam was used in the drainage modeling to describe the behavior of foam decay, which is presented in further detail below.

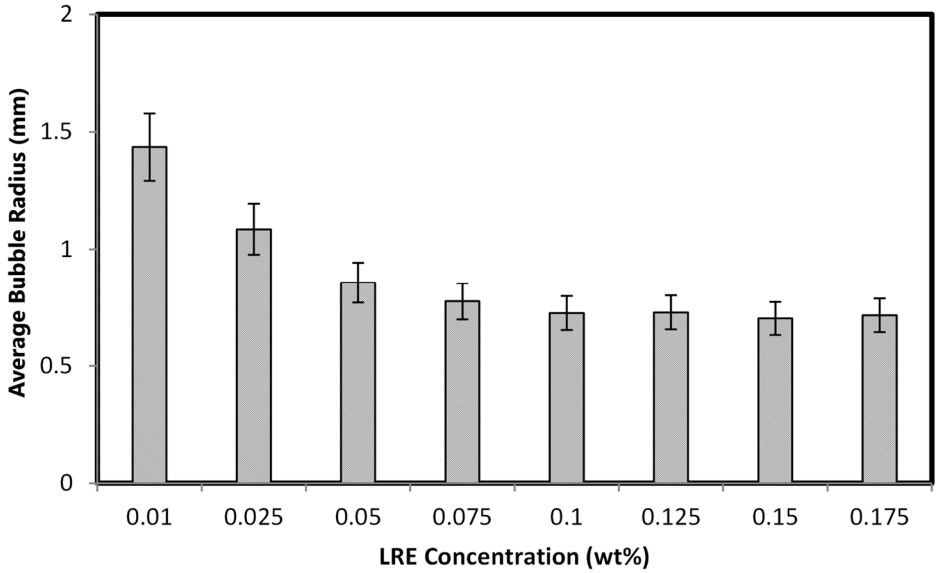

Figure 5. The average bubble radius at different LRE concentrations.

4.2. Drainage Estimated from Modeling and Experimental Data

The target of this investigation was to compare the drainage behavior of LRE foams with the simplified theoretical modeling, as presented above. In the experimental part, the amount of drained liquid was measured as a function of time until the foam was completely collapsed. As an example, six snapshots during the foam decay process for a sample LRE

solution (concentration of 0.15 wt%) are shown in Figure 6. In these photos, the dashed line shows the amount of liquid drained in the previous image to better understand the rate of drainage. It was experimentally observed that the drainage rate at the beginning of the process was higher.

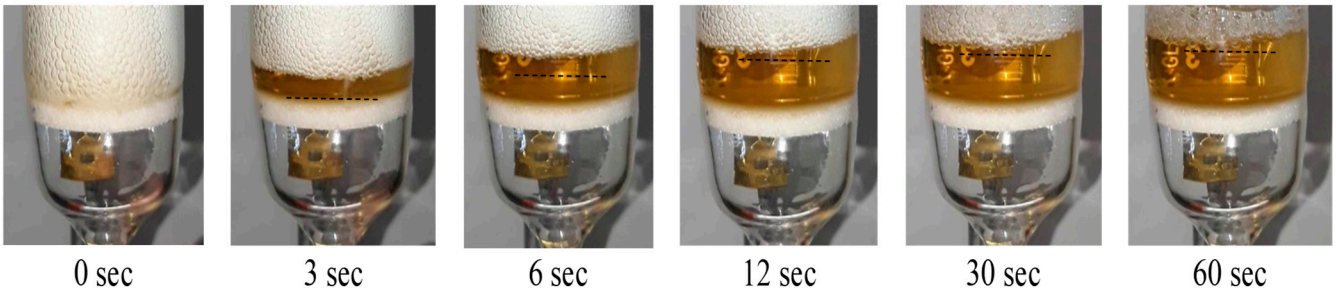

Figure 6. Images during the foam drainage for the LRE concentration of 0.15 wt%.

Figure 7 shows the time-dependent drainage data, together with the theoretical modeling results, for the foams generated from eight different LRE solutions (0.01, 0.025, 0.05, 0.075, 0.01, 0.0125, 0.015, and 0.0175 wt%). The drained volume is shown as a function of time normalized by the total volume drained from the foam, V_f. We can see that the observed drainage behavior is similar to the predicted curves obtained from the analytical solution of Equation (18) for $m = 1/2$. The initial drainage rate is high and approximately constant, followed by a reduction as the process continues. Adopting 0.5 for the index of the dissipation mechanism revealed that in the LRE foams, shear flow occurred in the junctions; accordingly, node dissipation was the dominant mechanism.

Foams prepared from solutions at low concentrations (0.01 and 0.025%) had a short life and disappeared in less than a minute, while for the foams obtained at higher concentrations, drainage due to foam film breakage took up to about 3 min. Consequently, the foam stability improved remarkably with increasing LRE concentration. This result was completely consistent with the values of the measured effective parameters. Reducing the bubble diameters (resulting from the decrease in surface tension) increased the drainage time and, hence, the stability of the foam. Therefore, it can be suggested that the stability of the foam is governed by the properties of the LRE solution. In addition, in [41], the authors proposed that forming bubbles with a smaller diameter leads to a decrease in the foam drainage rate. The greater stability of foam with smaller bubbles can be described based on bubble destabilization mechanisms. According to Stokes' law, a larger bubble diameter results in greater buoyancy and faster creaming. Consistent with their report, the experimental results of the present research also clearly show that foams with smaller bubble sizes have significantly slower drainage rates. These findings can be supported by our theoretical modeling (mathematical relationships).

In addition, it can be seen in Figure 7 that the drainage curves from both the experimental and the theoretical approaches were in fairly good agreement with each other and showed similar behavior. However, there is a slight difference between the experimental results and the analytical solution, which can be caused by the simplifying assumptions in the modeling and, finally, by solving the drainage equation. For example, assumptions such as the negligible flow in the films between bubbles and the removal of capillarity pressure effects can be reasons for the discrepancy. In addition, considering a completely uniform foam is an ideal supposition, which cannot occur in practice. Therefore, in the experiment, the drainage rate was a bit higher than the analytical solution obtained from the theoretical approach.

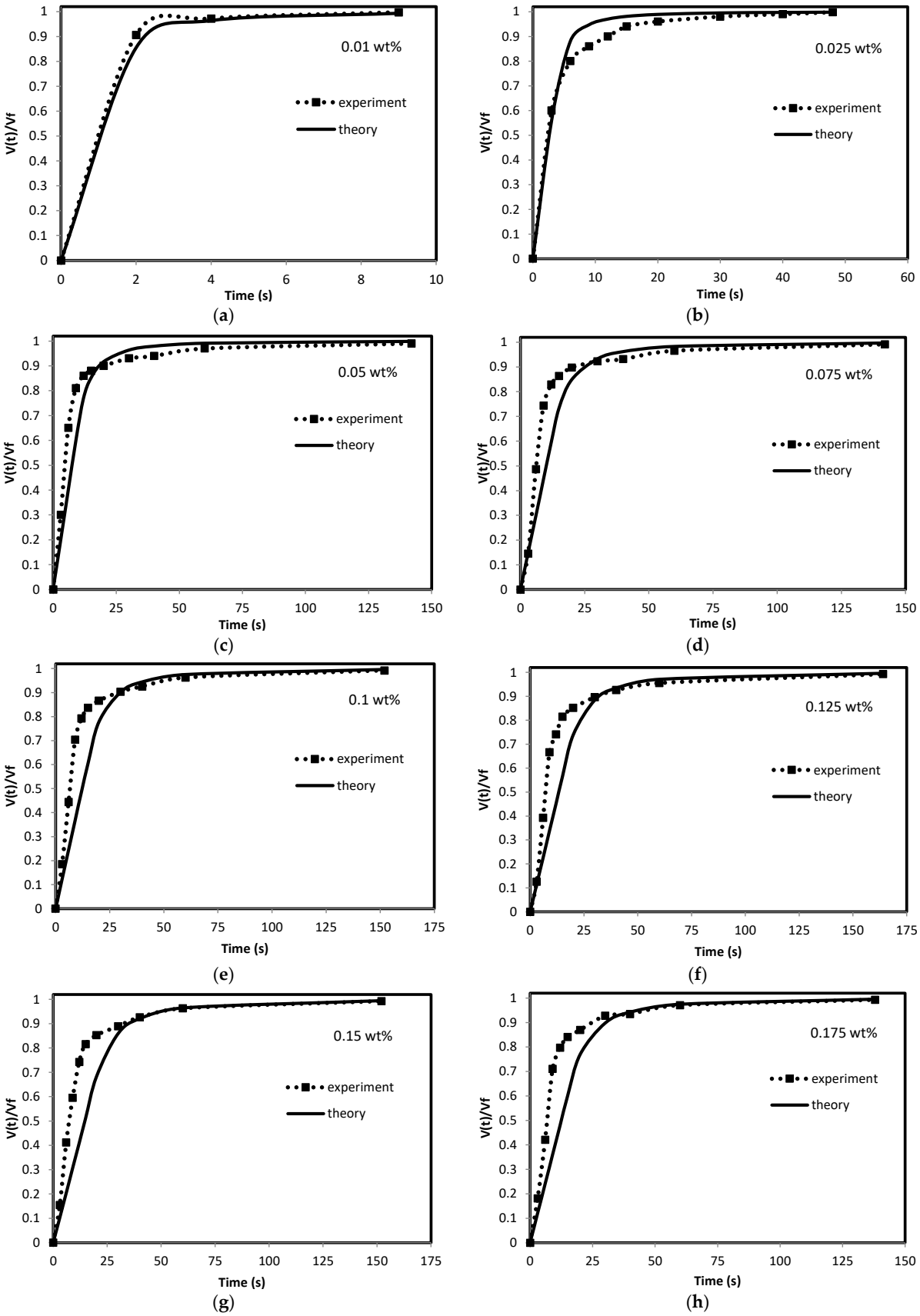

Figure 7. Comparison of measured drainage with theoretical modeling results for LRE foams at different concentrations of (**a**) 0.01, (**b**) 0.025, (**c**) 0.05, (**d**) 0.075, (**e**) 0.1, (**f**) 0.125, (**g**) 0.15, and (**h**) 0.175 wt%.

In order to examine the relationships obtained from the analytical solution of the drainage equation and the characterization of the effective parameters, the results are summarized in Table 2. Since the initial cross-sectional area of the channels is proportional to the square of the average bubble radius, larger bubbles increase the area of the channels. In addition, according to Equation (15), the maximum characteristic velocity has a direct relationship with density and an inverse relationship with viscosity. Consequently, increasing the density and the average size of the bubbles causes an increase in the maximum characteristic velocity, while increasing the viscosity of the liquid leads to a reduction in the drying front velocity of the foam. This prediction, which was obtained from the theoretical approach, was studied by the experimental method. For further explanation, it can be seen from Table 2 that foam with a smaller average radius (lower initial channel area) and higher viscosity has a lower drainage rate, which actually corresponds to a slower rate of the drying front. In addition, the constant velocity (see Equation (17)) is a more complete characteristic that includes the effects of the dissipation mechanism and the initial volume fraction of the liquid. The formula for defining this characteristic shows that wetter foams drain faster because of the larger liquid channels between the bubbles and exhibit a lower hydrodynamic resistance. In addition, v/h is another critical parameter that indicates the time for the change in the drainage rate behavior. After this inflection point, drainage takes place at slower rates due to the lack of liquid remaining in the foam. Furthermore, it was previously presented that the capillary length scales are defined based on a combination of surface tension and bubble size. As indicated in Table 2, the capillary length scales ranged from 0.029 to 0.032 cm. Subsequently, the minimum value of h/ζ was 10.3, meaning that it was reasonable to delete the capillary pressure term.

Table 2. Characteristics of foam drainage at different LRE concentrations.

LRE Concentration (wt%)	u_0 (cm/s)	v (cm/s)	v/h (s)	ζ (cm)	h/ζ
0.01	24.05	2.42	1.3	0.030	10.3
0.025	18.43	1.39	3.5	0.032	15.5
0.05	16.64	1.06	9.3	0.032	31.1
0.075	15.31	0.89	13.2	0.030	38.6
0.1	14.62	0.82	16.3	0.030	44.9
0.125	13.48	0.76	17.7	0.031	44.0
0.15	12.39	0.69	19.5	0.031	43.0
0.175	13.75	0.78	17.2	0.029	46.2

In order to further compare the theoretically predicted drainage rates with the experimental results, the drainage slopes at the beginning of the process from both methods are summarized in Table 3. The initial slope of the drainage process, $u_0\varepsilon_0^m/h$, can be introduced as a key characteristic to express the correlation of variables affecting the foam drainage by a mathematical relationship. These results are presented because foams are usually used in practical applications within a short time of their generation, so it is appropriate to control the initial drainage rate. As reported in this table, the slope of the drainage curves showed a relatively good agreement between experiment and theory. The results indicate that a lower drainage rate was observed for foams obtained with solutions of higher LRE concentrations ($C \geq 0.075$ wt%). Therefore, the LRE foam drainage can be predicted and described using a mathematical model derived from theoretical considerations. As a result, we can use this simplified theoretical model to quantitatively investigate the change in the effective parameters and estimate the stability of foams when manufacturing new commercial products.

Table 3. Comparison of experimental drainage with the theoretical approach.

Item	Values							
LRE Concentration (wt%)	0.01	0.025	0.05	0.075	0.1	0.124	0.15	0.175
Slope (modeling) (1/s)	0.504	0.186	0.071	0.050	0.041	0.037	0.035	0.040
Slope (experiment) (1/s)	0.453	0.201	0.087	0.048	0.049	0.041	0.043	0.051

5. Conclusions

In the present work, an explicit relationship for the volume of drained liquid under free drainage conditions by simplifying the standard foam drainage equation was obtained. Combinations of effective parameters appeared during the process of solving the drainage equation, which were considered as important characteristics related to the drainage rate to express the mathematical relationship between the effective factors. The experimental approach for measuring LRE foam drainage could be used to examine the results of the theoretical model. It was concluded that experiment and theory show similar behavior for the drainage as a function of time. The initial slope of the time-dependent drainage obtained from the theoretical approach is a complete combination of parameters suitable to describe drainage. Consequently, the presented theoretical model is suitable for estimating the free drainage of licorice root extract foam and, hence, to predict its stability. In addition, the relationships obtained from this modeling can be used to quantify the effects of changes in the effective parameters, including bubble size and the solution's surface tension, on foam drainage.

Author Contributions: Methodology, H.A.T.; validation, H.A.T.; formal analysis, H.A.T. and R.M.; investigation, H.A.T.; resources, H.A.T. and S.Y.; writing—original draft preparation, H.A.T. and R.M.; writing—review and editing, M.H.K., A.F. and S.Y.; supervision, M.H.K., A.F. and S.Y. All authors have read and agreed to the published version of the manuscript.

Funding: This research received no external funding.

Data Availability Statement: The data presented in this study are available on request from the corresponding author.

Conflicts of Interest: The authors declare no conflict of interest.

References

1. Cantat, I.; Cohen-Addad, S.; Elias, F.; Graner, F.; Höhler, R.; Pitois, O.; Rouyer, F.; Saint-Jalmes, A. *Foams: Structure and Dynamics*; OUP Oxford: Oxford, UK, 2013; pp. 17–74.
2. Saint-Jalmes, A.; Langevin, D. Time evolution of aqueous foams: Drainage and coarsening. *J. Condens. Matter Phys.* **2002**, *14*, 9397. [CrossRef]
3. Pitois, O. *Foam ripening. Foam Engineering: Fundamentals and Applications*; John Wiley & Sons: Hoboken, NJ, USA, 2012; pp. 59–73.
4. Wang, J.; Nguyen, A.V.; Farrokhpay, S. A critical review of the growth, drainage and collapse of foams. *Adv. Colloid Interface Sci.* **2016**, *228*, 55–70. [CrossRef] [PubMed]
5. Koehler, S.A.; Hilgenfeldt, S.; Stone, H.A. A generalized view of foam drainage: Experiment and theory. *Langmuir* **2000**, *16*, 6327–6341. [CrossRef]
6. Weaire, D.; Hutzler, S.; Verbist, G.; Peters, E. A review of foam drainage. *Adv. Chem. Phys.* **1997**, *102*, 315–374.
7. Magrabi, S.; Dlugogorski, B.; Jameson, G. Free drainage in aqueous foams: Model and experimental study. *AICHE J.* **2001**, *47*, 314–327. [CrossRef]
8. Saint-Jalmes, A.; Vera, M.; Durian, D. Uniform foam production by turbulent mixing: New results on free drainage vs. liquid content. *Eur. Phys. J. B* **1999**, *12*, 67–73. [CrossRef]
9. Papara, M.; Zabulis, X.; Karapantsios, T.D. Container effects on the free drainage of wet foams. *Chem. Eng. Sci.* **2009**, *64*, 1404–1415. [CrossRef]
10. Weaire, D.; Pittet, N.; Hutzler, S.; Pardal, D. Steady-state drainage of an aqueous foam. *Phys. Rev. Lett.* **1993**, *71*, 2670. [CrossRef]
11. Hutzler, S.; Weaire, D. Foam coarsening under forced drainage. *Philos. Mag. Lett.* **2000**, *80*, 419–425. [CrossRef]
12. Stevenson, P. On the forced drainage of foam. *Colloids Surf. A Physicochem. Eng. Asp.* **2007**, *305*, 1–9. [CrossRef]
13. Koehler, S.; Stone, H.; Brenner, M.; Eggers, J. Dynamics of foam drainage. *Phys. Rev. E* **1998**, *58*, 2097. [CrossRef]
14. Sun, Q.; Tan, L.; Wang, G. Liquid foam drainage: An overview. *Int. J. Mod. Phys. B* **2008**, *22*, 2333–2354. [CrossRef]

15. Koehler, S.; Hilgenfeldt, S.; Stone, H. Foam Drainage in 2D: Comparison of Experiment and Theory. In Proceedings of the APS Division of Fluid Dynamics Meeting Abstracts, New Orleans, LA, USA, 21–23 November 1999.
16. Koehler, S.; Hilgenfeldt, S.; Stone, H. Flow along two dimensions of liquid pulses in foams: Experiment and theory. *Europhys. Lett.* **2001**, *54*, 335. [CrossRef]
17. Kitagawa, I. Licorice root. A natural sweetener and an important ingredient in Chinese medicine. *Pure Appl. Chem.* **2002**, *74*, 1189–1198. [CrossRef]
18. Karaoğul, E.; Parlar, P.; Parlar, H.; Alma, M.H. Enrichment of the glycyrrhizic acid from licorice roots (*Glycyrrhiza glabra* L.) by isoelectric focused adsorptive bubble chromatography. *J. Anal. Chem.* **2016**, *2016*, 7201740.
19. Asl, M.N.; Hosseinzadeh, H. Review of pharmacological effects of Glycyrrhiza sp. and its bioactive compounds. *Phytother. Res. Int. J. Devoted Pharmacol. Toxicol. Eval. Nat. Prod. Deriv.* **2008**, *22*, 709–724.
20. Kamei, J.; Saitoh, A.; Asano, T.; Nakamura, R.; Ichiki, H.; Iiduka, A.; Kubo, M. Pharmacokinetic and pharmacodynamic profiles of the antitussive principles of Glycyrrhizae radix (licorice), a main component of the Kampo preparation Bakumondo-to (Mai-men-dong-tang). *Eur. J. Pharmacol.* **2005**, *507*, 163–168. [CrossRef]
21. Fiore, C.; Eisenhut, M.; Ragazzi, E.; Zanchin, G.; Armanini, D. A history of the therapeutic use of liquorice in Europe. *J. Ethnopharmacol.* **2005**, *99*, 317–324. [CrossRef]
22. El-Lahot, A.; El-Razek, A.; Amal, M.; Massoud, M.I.; Gomaa, E. Utilization of glycyrrhizin and licorice extract as natural sweetener in some food products and biological impacts. *J. Food Dairy Sci.* **2017**, *8*, 127–136. [CrossRef]
23. Mardani, M.; Yeganehzad, S.; Niazmand, R. Structure–function relationship of licorice (*Glycyrrhiza glabra*) root extract–xanthan/guar gum mixture in a high sugar content system. *J. Sci. Food Agric.* **2022**, *102*, 1056–1065. [CrossRef]
24. Chen, J.; Lin, Y.; Wu, M.; Li, C.; Cen, K.; Liu, F.; Liao, Y.; Zhou, X.; Xu, J.; Cheng, Y. Glycyrrhetinic acid proliposomes mediated by mannosylated ligand: Preparation, physicochemical characterization, environmental stability and bioactivity evaluation. *Colloids Surf. B Biointerfaces* **2022**, *218*, 112781. [CrossRef]
25. Isbrucker, R.; Burdock, G. Risk and safety assessment on the consumption of Licorice root (*Glycyrrhiza* sp.), its extract and powder as a food ingredient, with emphasis on the pharmacology and toxicology of glycyrrhizin. *Regul. Toxicol. Pharmacol.* **2006**, *46*, 167–192. [CrossRef] [PubMed]
26. İbanoğlu, E.; İbanoğlu, Ş. Foaming behaviour of liquorice (*Glycyrrhiza glabra*) extract. *Food Chem.* **2000**, *70*, 333–336. [CrossRef]
27. Böttcher, S.; Drusch, S. Interfacial properties of saponin extracts and their impact on foam characteristics. *Food Biophys.* **2016**, *11*, 91–100. [CrossRef]
28. Patriche, S.; Grigoraș, C.; Barbu, V.; Dinică, R.M.; Cârâc, G.C. Antioxidative activity and stability of the extracts of liquorice root (*Glycyrrhiza glabra*). *Ann. Univ. Dunarea Jos Galati Fascicle VI Food Technol.* **2015**, *39*, 77–87.
29. Larson, R.; Higdon, J. A periodic grain consolidation model of porous media. *Phys. Fluids A Fluid Dyn.* **1989**, *1*, 38–46. [CrossRef]
30. Gol'Dfarb, I.; Kann, K.; Shreiber, I. Liquid flow in foams. *Fluid Dyn.* **1988**, *23*, 244–249. [CrossRef]
31. Kraynik, A.M. *Foam Drainage*; Sandia National Labs: Albuquerque, NM, USA, 1983.
32. Anazadehsayed, A.; Naser, J. A combined CFD simulation of Plateau borders including films and transitional areas of liquid foams. *Chem. Eng. Sci.* **2017**, *166*, 11–18. [CrossRef]
33. Alquran, M. Analytical solutions of fractional foam drainage equation by residual power series method. *Math. Sci.* **2014**, *8*, 153–160. [CrossRef]
34. Holmberg, K.; Shah, D.O.; Schwuger, M.J. *Handbook of Applied Surface and Colloid Chemistry*; John Wiley & Sons: Hoboken, NJ, USA, 2002; Volume 2, pp. 23–45.
35. Vatanparast, H.; Samiee, A.; Bahramian, A.; Javadi, A. Surface behavior of hydrophilic silica nanoparticle-SDS surfactant solutions: I. Effect of nanoparticle concentration on foamability and foam stability. *Colloids Surf. A Physicochem. Eng. Asp.* **2017**, *513*, 430–441. [CrossRef]
36. Dorman, H.; Peltoketo, A.; Hiltunen, R.; Tikkanen, M. Characterisation of the antioxidant properties of de-odourised aqueous extracts from selected Lamiaceae herbs. *Food Chem.* **2003**, *83*, 255–262. [CrossRef]
37. Tighchi, H.A.; Kayhani, M.H.; Faezian, A.; Yeganehzad, S.; Miller, R. Dynamic interfacial properties and foam behavior of licorice root extract solutions. *Colloids Surf. B Biointerfaces* **2023**, *224*, 113181. [CrossRef] [PubMed]
38. Schneider, C.A.; Rasband, W.S.; Eliceiri, K.W. NIH Image to ImageJ: 25 years of image analysis. *Nat. Methods* **2012**, *9*, 671–675. [CrossRef] [PubMed]
39. Ptaszek, P.; Kabziński, M.; Kruk, J.; Kaczmarczyk, K.; Żmudziński, D.; Liszka-Skoczylas, M.; Mickowska, B.; Łukasiewicz, M.; Banaś, J. The effect of pectins and xanthan gum on physicochemical properties of egg white protein foams. *J. Food Eng.* **2015**, *144*, 129–137. [CrossRef]
40. Faezian, A.; Yeganehzad, S.; Tighchi, H.A. A simplified model to describe drainage of egg white powder foam containing additives. *Chem. Eng. Sci.* **2019**, *195*, 631–641. [CrossRef]
41. Lomakina, K.; Mikova, K. A study of the factors affecting the foaming properties of egg white-a review. *Czech J. Food Sci.* **2006**, *24*, 110–118. [CrossRef]